



On the cracking patterns of brittle rings with elastic radial support under hydrostatic pressure

Sébastien Michel · András A. Sipos

Received: 27 November 2021 / Accepted: 29 March 2022 / Published online: 26 April 2022
© The Author(s) 2022

Abstract The evolution of the cracking pattern of an internally pressurized, circular, brittle ring supported with radial elastic springs is investigated. The ill-posed Griffith-type energy functional is regularized via a sequence of boundary value problems (BVPs). We show, that internal bending in the fragments plays an essential role in the position of the new crack. We also find that the pattern formation is driven by a co-dimension one bifurcation, which leads to the conclusion that in the beginning of the cracking process the new crack emerges in the vicinity of the existing cracks. In the second phase of the evolution the cracking process obeys a halving rule. The critical value of the fragment-length is derived. The results obtained are readily applicable to describe the crack evolution of hemispherical domes.

Keywords Brittle ring · Griffith energy · Pattern bifurcation · Cracking pattern

S. Michel
Department of Mechanics, Materials and Structures,
Budapest University of Technology and Economics,
Budapest, Hungary
e-mail: sebastien.michel@edu.bme.hu

A. A. Sipos (✉)
Department Morphology and Geometric Modeling &
MTA-BME Morphodynamics Research Group, Budapest
University of Technology and Economics, Budapest,
Hungary
e-mail: siposa@eik.bme.hu

Nomenclature

Problem unknowns	
$\Delta\kappa$	Curvature variation
Γ	Cracked set
ν	Hoop strain
v	Tangential displacement
w	Radial displacement
Physical parameters	α
	Dimensionless spring rigidity
β	Dimensionless rigidity
χ	Relaxation parameter value
η, ζ	Characteristic numbers of the problem
γ	Dimensionless fracture toughness
λ	Slenderness of the ring
A	Area of the ring's cross-section
E	Young's modulus
G	Fracture toughness
I	Moment of inertia of the ring's cross-section
k_v	Tangential rigidity of the support
k_w	Radial rigidity of the support
p	Internal pressure

1 Introduction

Investigating the cracking pattern plays a prominent role in different fields of science, think about stress-inversion methods in structural geology [1], or the stimulating history of the cracks of the St. Peter's Basilica in Vatican City [2]. Starting with the seminal paper by Griffith [3], a flourishing literature has been devoted to the subject of quantifying and predicting the fracture process, but none of the methods currently available has yet proved to be unanimously adopted. At one end of the spectrum, the classical continuum mechanics approach relies on the local study of the singular stress field around the crack extremities. This stress field is studied by various regularization tricks allowing to retrieve the singularity at the crack tip as some limit. Refinements of the material behavior around the crack tip, taking into account some level of plasticity, relaxation or cohesive zones coupled with an ad-hoc yield criterion allows to rule out unphysical energy values while accounting for the real properties of the material: it can be decided if, how and where the crack would behave [4, 5]. A limitation in this class of models is to handle the initiation of the crack: the a-priori existence of a singularity is a needed ingredient to tackle the problem.

On the other side attempts to provide a unified framework of fracture roots into a variational framework [6–9]. The energy of a sample is considered as the sum of a bulk energy for the uncracked parts and a fracture energy and a functional is minimized over both a deformation field on the cracked body and a test crack set modifying the geometry of the body, whose choice is conditioned by some dissipation potential. The whole evolution of the cracking is then reduced to a sequence of minimization problems over some functional space. Properties of the crack evolution can be decided depending on the properties of the functional chosen, and the irreversibility of the cracking has to be enforced via additional unilateral constraints on the problem. The unified framework offered provides a single criterion for crack study regardless if it is question of tackling initiation, growth or pattern of the crack.

Despite the long track record of the study of crack formation and fracture mechanics, the connection between the fracture process and the emerging geometric pattern is still partially unrevealed.

Most of the relevant literature focuses on the growth of a *single crack* under external loading. The developed cracking pattern is also widely studied, both with the techniques of classical mechanics [5], statistical physics [10] and pure geometry [11]. The classical problem of the unexpected meridional cracking of the St. Peter's Basilica in Rome [2, 12] underscores the validity of investigating the equilibrium and overall mechanical performance of the cracked structure without considering the evolutionary path that produced the pattern itself. Motivated by the distinguished role of hemispherical domes made of materials with limited tensile strength (i.e., masonry, concrete) in structural mechanics [2, 13], this study aims to introduce a simple model based on *dimension-reduction*, that can describe the evolution of the emergence of new cracks as the external load is increased. In specific, instead of a hemispherical dome, a pressurized, brittle ring with elastic supports, associated with a horizontal section closed to the bottom of the dome, is considered. The evolution of the pattern, that covers the mutual effect of the existing cracks on each other and the emerging new crack requires to follow the time-development of the system, where cracks produce sudden jumps in the displacement field. Due to the simplified geometry, analytical treatment of the problem is possible, as long as the elasticity of the support is constant along the perimeter of the ring. Although we start with postulating the potential energy of the system, instead of introducing a damage-field to regularize the ill-posed functional, the one-dimensional setting enables us to follow a sequence of boundary value problems (BVP). Each BVP is associated with an unbroken fragment of the ring, where, upon fragmentation, the elastic energy is relaxed. Furthermore, an energetic condition is used to determine the position of the new crack along with the critical load needed for such an event.

The paper is organized as follows. The model assumptions and the governing equations are introduced in Sect. 2. Assuming constant support rigidity the model is studied analytically in Sect. 3. The following Sect. 4 is devoted to numerical results, in particular imperfections are introduced via a spatially varied strength of the support. Finally, conclusions are drawn.

2 Model development

Consider a closed, circular ring with radius R in the plane with a polar parametrization with respect to the central angle $\theta \in [0, 2\pi]$ (see Fig. 1, left). The curved rod is assumed to be unshearable, hence its elastic behavior is characterized by the flexural rigidity EI and the extensional rigidity EA , where both are assumed to be constant along the arc length. Here E stands for the modulus of elasticity, I is the second moment of area and A denotes the area of the cross-section. The ring is linked to a support exerting a spring-like reactions in both the tangential direction $\mathbf{t}(\theta)$ and radial direction $\mathbf{n}(\theta)$, with respective stiffnesses k_v and k_w . It is loaded by a constant inner pressure p directed to the outward normal $\mathbf{n}(\theta)$. Finally we consider that the ring is made of a brittle material of fracture toughness G . In our model we consider planar deformations (i.e., out-of-plane displacements are not allowed) with radial component $w(\theta)$ and tangential component $v(\theta)$. We assume that any initiated crack rapidly extends the entire cross-section of the beam, hence we only allow for fully cracked or non-cracked cross-sections, and exclude partial cracking. We assume sufficient internal damping and the dissipated energy associated with damping is included in the fracture energy. This latest assumption allows us to follow a *quasi-static* approach, in which a sequence of equilibrium states are studied and contributions from dynamic effects are neglected.

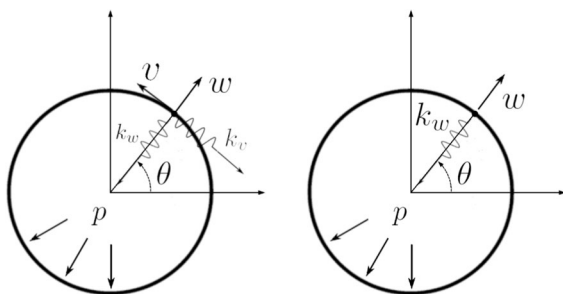


Fig. 1 The general model of an internally pressurized ring constrained to the plane and supported by radial and tangential springs and displacement components v and w , respectively (left). In the simplified model $v \equiv 0$, hence only radial movements are allowed (right)

2.1 The energy functional

Let Ω denote the reference domain associated with the problem. Our problem can be formulated in the framework of the classical energy-based approach of brittle fracture of [3] as the minimization over admissible displacement fields v, w and cracked sets Γ of the following energy functional:

$$\mathcal{E}(\theta, v, w, \Gamma(\theta)) = \int_{\Omega} \left\{ \frac{1}{2}(k_v v^2 + k_w w^2) - pw \right\} + \int_{\Omega \setminus \Gamma(\theta)} \Phi(\cdot) + \int_{\Gamma(\theta)} GA, \tag{1}$$

where the first term on the right-hand side accounts for the work of the internal pressure and the elastic energy of the supporting springs, the second integral is the bulk energy in the unbroken part of the ring and the last term is the fracture energy associated with the (brittle) cracks. The main hardness here stems from the explicit dependence of the functional on the cracked set $\Gamma(\theta)$ with zero measure. In specific, let N denote the number of the cracks and θ_i^N ($i = 1, \dots, N$) represent the position of the cracks. Then $\Gamma(\theta) := \{\theta_1^N, \dots, \theta_N^N\}$. Without loss of generality $\theta_1^N = 0$ is postulated. Note that any unbroken fragment can be identified by its starting and ending angle, i.e., $[\theta_i^N, \theta_{i+1}^N]$, where, because of the rotational nature of the problem, the convention $\theta_{N+1}^N = \theta_1^N$ is adopted, which means, that the last fragment is labeled by $[\theta_N^N, \theta_1^N]$.

As $\Gamma(\theta)$ is a set with measure zero, the minimization problem that contains functional (1) is *ill-posed*. On the one hand one can investigate the problem as the union of uncracked segments and book keep the energy absorbed in the cracking process. Here a series of Boundary Value Problems (BVPs) can be associated with the problem. Classical regularization techniques can resolve the ill-posedness, such techniques are called *variational brittle fracture* in the literature [6, 14, 15]. Note that variational brittle fracture is a general framework for 2D or 3D manifolds. There the damage field used for the regularization is associated with the internal stress, while in a 1D setting (i.e., a rod theory) it should be associated with the internal actions on the cross-section of the rod. Although there exist rod models along the lines of variational brittle fracture [16], in our case it seems more natural

to keep the energy functional (1) and carry out minimization with respect to the unknown fields and the discrete set of the crack positions directly.

In order to complete the model, we need the elastic energy density $\Phi(\cdot)$. A classical, finite strain model could be derived along the arc length parametrization of the shape [17]. As we are interested in brittle fragmentation, a simple, linear model for the elastic behavior of the unbroken segments of the ring is adopted. The v normal strain and $\Delta\kappa$ change of curvature comprise the strain variables of the model and simple geometric considerations yield

$$v = \frac{w + v_{,\theta}}{R}, \tag{2}$$

$$\Delta\kappa = \frac{w + w_{,\theta\theta}}{R^2}. \tag{3}$$

Note that we denote differentiation with respect to a variable with a coma-separated subscript. For instance the derivative of $f_a(b, c)$ w.r.t. b and c reads $f_{a,bc} = \partial_b \partial_c f_a$. Now the strain energy density Φ reads

$$\begin{aligned} \Phi(v, \Delta\kappa) &= \frac{1}{2}EA v^2 + \frac{1}{2}EI \Delta\kappa^2 \\ &= \Phi(v, w, w_{,\theta\theta}) \\ &= \frac{1}{2}EA \left(\frac{w + v_{,\theta}}{R} \right)^2 + \frac{1}{2}EI \left(\frac{w + w_{,\theta\theta}}{R^2} \right)^2. \end{aligned} \tag{4}$$

Here we seek the simplest model to predict the cracking patterns of the ring, hence in the following $k_v \rightarrow \infty$ and consequently $v \equiv 0$ is assumed (see Fig. 1, right). On the one hand this assumption reduces the unknown displacement fields to one, on the other hand it excludes shortening of the ring in case of cracking. In other words, the ring cannot exhibit relaxation upon cracking. To mimic relaxation, we assume that the elastic energy of any unbroken part $[\theta_i^N, \theta_{i+1}^N]$ also depends on the number of the cracking events, needed to form the fragment in question. If a new crack forms in a fragment associated with $1 \leq i^* \leq N$, at $\theta_i^N \leq \theta^* \leq \theta_{i+1}^N$, then

$$\theta_i^{N+1} = \begin{cases} \theta_i^N & \text{if } i \leq i^*, \\ \theta^* & \text{if } i = i^* + 1, \\ \theta_{i-1}^N & \text{if } i > i^* + 1. \end{cases} \tag{5}$$

Let k_i^N be an integer that counts the cracking events needed to produce the fragment $[\theta_i^N, \theta_{i+1}^N]$. The following iterative process starts with a ring containing a single crack at $k_1^1 = 1$. If a new crack forms in a fragment associated with $1 \leq i^* \leq N$, then

$$k_i^{N+1} = \begin{cases} k_i^N & \text{if } i < i^*, \\ k_i^N + 1 & \text{if } i = i^*, \\ k_i^N + 1 & \text{if } i = i^* + 1, \\ k_{i-1}^N & \text{if } i > i^* + 1. \end{cases} \tag{6}$$

Applying k_i^N , the elastic energy of the unbroken fragment reads

$$\begin{aligned} \Phi_i^N(w, w_{,\theta\theta}, k_i^N) \\ = \chi(k_i^N) \left(\frac{1}{2}EA \left(\frac{w}{R} \right)^2 + \frac{1}{2}EI \left(\frac{w + w_{,\theta\theta}}{R^2} \right)^2 \right), \end{aligned} \tag{7}$$

where $0 < \chi(k_i^N) \leq 1$ is some *relaxation function* and due to our assumptions Φ becomes dependent on w and k_i^N . In our setup we will assume that the relaxation takes place only in the fragment undergoing cracking, and that the relaxation is linear in the number of cracking events that were necessary to create the fragment. In specific, we define $\chi(k_i^N)$ via

$$\chi(k) = \max(1 - k\delta\chi, 0). \tag{8}$$

with $\delta\chi > 0$ being a small, fixed relaxation parameter. That is the relaxation function decreases slightly on the two fragments that are formed in the cracking event.

The internal normal force F_i^N , bending moment M_i^N and shear force V_i^N in the unbroken fragment are directly obtained:

$$F_i^N = \chi(k_i^N)EA v = \frac{EA}{R} w, \tag{9}$$

$$M_i^N = \chi(k_i^N)EI \Delta\kappa = \frac{EI}{R^2} (w + w_{,\theta\theta}), \tag{10}$$

$$V_i^N = M_{i,s}^N = -M_{i,\theta}^N \frac{d\theta}{ds} = -\chi(k_i^N) \frac{EI}{R^3} (w + w_{,\theta\theta})_{,\theta}. \tag{11}$$

Note that a rigorous derivation of F_i^N [18] results in a slightly different expression, however, we do not use F_i^N in the following derivation, hence keep the approximation above.

2.2 Non-dimensional formulation

In order to simplify the following formulas, we introduce non-dimensional parameters. We assume a square cross-section for the ring with identical height and width denoted to h . Let the λ slenderness of the ring be defined as $\lambda := Rh^{-1}$. Similarly, let $\alpha := k_w E^{-1}$ and $\beta := p(Eh)^{-1}$ and $\gamma := G(hE)^{-1}$. With this in hand we observe that

$$\frac{EAR^2}{EI} = \frac{Eh^2R^2}{Eh^4/12} = 12\lambda^2, \tag{12}$$

$$\frac{k_wR^4}{EI} = \frac{k_w}{E} \frac{R^4}{h^4/12} = 12\alpha\lambda^4, \tag{13}$$

$$\frac{pR^4}{EI} = \frac{p}{Eh} \frac{R^4}{h^3/12} = 12\beta\lambda^3R, \tag{14}$$

$$\frac{GAR^4}{EI} = \frac{G}{Eh} \frac{h^2R^4}{h^3/12} = 12\gamma\lambda R^3. \tag{15}$$

Scaling w and ε with R and using the fact, that the ds infinitesimal arch length in polar coordinates reads $ds = Rd\theta$, we obtain the non-dimensional form of the energy functional:

$$\begin{aligned} \mathcal{E}(w, \Gamma(\theta)) &= \int_0^{2\pi} \{6\alpha\lambda^4w^2 - 12\beta\lambda^3w\}d\theta \\ &+ \chi(k_1^N) \int_{\theta_1=0}^{\theta_2} \left\{6\lambda^2w^2 + \frac{1}{2}(w + w_{,\theta\theta})^2\right\}d\theta \\ &+ \dots + \chi(k_N^N) \int_{\theta_N}^{2\pi} \left\{6\lambda^2w^2 + \frac{1}{2}(w + w_{,\theta\theta})^2\right\}d\theta \\ &+ \sum_{i=1}^N 12\gamma\lambda. \end{aligned} \tag{16}$$

Considering a ring made of a concrete-like material and a diameter around 40m, the relevant range of the non-dimensional parameters are found to be $10^{-9} \leq \alpha \leq 10^{-7}$, $10^{-7} \leq \beta \leq 10^{-5}$, $10^{-9} \leq \gamma \leq 10^{-7}$ and $5 \leq \lambda \leq 50$.

In the following, the energy associated with the elastic components of the system (bulk energy) is denoted to Ψ . It reads

$$\Psi(w, \Gamma(\theta)) := \mathcal{E}(w, \Gamma(\theta)) - \sum_{i=1}^N 12\gamma\lambda. \tag{17}$$

In the next section we investigate the perfect problem with k_w , hence α assumed to be constant along the perimeter of the ring.

3 Cracking pattern formation

3.1 An existence result

Here we justify the existence of minimizers of the functional in (1). This kind of problem roots in image segmentation [19, 20] and has been labeled as a *free discontinuity problem* in the literature. In our setup the functional is second order, which differs slightly from the one considered in Francfort and Marigo’s book [6]. Nonetheless, the existence of a minimizer can be rigorously proved by using a Γ -convergence approximation argument, and the adapted function space called the Generalized Special Functions of Bounded Variations, GSBV in short. A first version of the result was proved by Belletini [21] and generalized further by Ambrosio [22].

To place ourselves in the latter setup, we consider the minimization problem (1) after leaving out the tangential displacement field v . We follow the steps given by Ambrosio [22] to show Γ -convergence. We consider the minimization of the following energy functional:

$$\begin{aligned} \mathcal{E}(w, \Gamma) &= \int_0^{2\pi} \left(6\lambda^2\alpha w^2 - 12\beta\lambda^3w + \frac{\chi}{2}(w + w_{,\theta\theta})^2\right. \\ &\quad \left.+ 6\chi\lambda^2w^2\right)d\theta + \int_{\Gamma} GA. \end{aligned} \tag{18}$$

The integrand of the first term defines an elliptic parabo-loid so up to a simple coordinate change the problem is the minimization of some Blake-Zisserman functional. To get rid of the dependence on the set Γ , we will consider functional spaces allowing discontinuities in the functions. We denote by $\mathcal{L}^n([0, 2\pi])$ the set of functions whose n -th power is integrable over $[0, 2\pi]$, and by $W^{k,p}([0, 2\pi])$ the Sobolev space of \mathcal{L}^p functions with generalized derivatives till order k in \mathcal{L}^p . Finally let $\tilde{w} \in GSBV([0, 2\pi]) \cap \mathcal{L}^2$, let $S(\tilde{w})$ denote the set of discontinuities of \tilde{w} and \mathcal{H}^0 the Hausdorff measure of dimension zero. We look at the minimization of the equivalent functional, after changing the coordinates:

$$F(\tilde{w}) = \int_0^{2\pi} \left(\tilde{w}_{,\theta\theta}^2 + C_1 \tilde{w}^2 \right) d\theta + C_2 \mathcal{H}^0(S_{\tilde{w}} \cup S_{\tilde{w},\theta}), \tag{19}$$

where C_1 and C_2 are constants that can be computed from the material parameters and the value of the relaxation χ . To regularize this functional we need to introduce some kind of approximation of the discontinuities. Using Ambrosio’s notation, we define for $s \in W^{1,2}([0, 2\pi]; [0, 1])$ and $\varepsilon > 0$

$$\mathcal{G}_\varepsilon(s) = \int_0^{2\pi} \left(\varepsilon s_{,\theta}^2 + \frac{1}{4\varepsilon} s^2 \right) d\theta. \tag{20}$$

Here s can be understood as some kind of damage field, whose value as the approximation takes place will be 1 at the cracking points and 0 everywhere else. We are now ready to introduce the approximating functional. For $\tilde{w} \in W^{2,2}([0, 2\pi])$ and $s \in W^{1,2}([0, 2\pi])$ we let

$$F_\varepsilon(\tilde{w}, s) = \int_0^{2\pi} \left((1 - s)^2 + \kappa_\varepsilon \right) w_{,\theta\theta}^2 + C_1 \tilde{w}^2 d\theta + C_2 \mathcal{G}_\varepsilon(s). \tag{21}$$

Let $X([0, 2\pi]) = \mathcal{L}^2([0, 2\pi]) \times \mathcal{L}^\infty([0, 2\pi], [0, 1])$. We extend the functionals over this wider space. We define $\mathcal{F} : X([0, 2\pi]) \rightarrow [0, +\infty]$ as:

$$\mathcal{F}(\tilde{w}, s) = \begin{cases} F(\tilde{w}) & \text{if } \tilde{w} \in GSBV([0, 2\pi]), s \equiv 0, \\ +\infty & \text{otherwise,} \end{cases} \tag{22}$$

and $\mathcal{F}_\varepsilon : X([0, 2\pi]) \rightarrow [0, +\infty]$ as:

$$\mathcal{F}_\varepsilon(\tilde{w}, s) = \begin{cases} F_\varepsilon(\tilde{w}, s) & \text{if } \tilde{w} \in GSBV([0, 2\pi]), s \equiv 0, \\ +\infty & \text{otherwise.} \end{cases} \tag{23}$$

Furthermore, we need to specify some additional properties for the infinitesimals in the approximation. We require $\kappa_\varepsilon > 0$ and $\kappa_\varepsilon = o(\varepsilon^4)$ as $\varepsilon \rightarrow 0$. We formulate the Γ -convergence result similarly to Ambrosio [22] although the problem is in the scope of [21].

Lemma 1 *With the previous assumptions, $(\mathcal{F}_\varepsilon)$ Γ -converges to \mathcal{F} in the $[\mathcal{L}^1([0, 2\pi])]^2$ topology as $\varepsilon \rightarrow 0$. Further, any limit point is of the form $(\tilde{w}, 0)$ with \tilde{w} a minimizer of E .*

Proof The approximation we constructed follows all the steps of Ambrosio [22, Section 3]. Moreover

our domain $\Omega = [0, 2\pi]$ is star-shaped. We get the full Γ -convergence result from Ambrosio’s Theorems 3.2 and 3.4. The fact that the limit point is a minimizer of F follows from the properties of the Γ -convergence □

3.2 Properties of the unbroken solutions

In this subsection we look at the equilibrium equations obtained from minimizing the functional with a given number of cracks N . We show that the problem of finding sequentially the position of new cracks reduces to a sequence of segmentation problems that can be solved explicitly. We also show that the sequence of problems defines a cracking criterion allowing to predict at which pressure threshold a new crack will occur.

We start with fixing the cracked domain $\Gamma(\theta)$ in the functional (16) and consider N cracks. Due to the rotational symmetry, the number of the fragments is also N . Investigating test displacement fields of the shape $\mathbb{1}_{(\theta_i^N, \theta_{i+1}^N)} w$ with $\theta_i^N, \theta_{i+1}^N \in \Gamma$, by using the classical tools of calculus of variations, we obtain that on each unbroken interval $[\theta_i^N, \theta_{i+1}^N]$ minimizing displacement fields satisfy the following ODE

$$\chi(k_i^N) \left(w_{,\theta\theta\theta\theta} + 2w_{,\theta\theta} + (1 + 12\lambda^2)w \right) + 12\alpha\lambda^4 w - 12\beta\lambda^3 = 0, \tag{24}$$

irrespective of the position of the ends of the unbroken section. Further we require the solution to satisfy the following boundary conditions at the ends of the domain

$$(w + w_{,\theta\theta})(\theta_i^N) = (w + w_{,\theta\theta})(\theta_{i+1}^N) = 0, \tag{25}$$

$$(w + w_{,\theta\theta})_{,\theta}(\theta_i^N) = (w + w_{,\theta\theta})_{,\theta}(\theta_{i+1}^N) = 0, \tag{26}$$

expressing respectively that the internal moment M_i^N (see (10)) and shear force V_i^N (see (11)) vanish at the broken ends of the fragment. Beyond being physical, these expressions produce uncoupled BVP-s, i.e., each segment can be solved in its own, as the boundary conditions are not effected by the neighboring fragments. Finally, we notice that the linear BVP given in (24), (25) and (26) is translation invariant as long as α is constant: solutions on identical length intervals are identical up to a translation.

From the translation invariance, we consider the BVP given above as follows. We denote the central angle of an unbroken piece by T , and consider that the unbroken piece is $[-T/2, T/2]$. Of course the boundary conditions (25), (26) are adapted and are taken at $\theta = \pm T/2$. It is easy to see that the BVP is well-posed hence defines a unique displacement field for almost all lengths T . From the system to solve, we also see that the solutions depends continuously on the parameter T , except maybe at points where it is not defined.

Solving the characteristic polynomial of (24) yields four complex roots. By the symmetry of the problem and basic algebraic manipulations it is clear that the solution can be written as the sum of a particular solution W_0 and a linear combination of the functions W_1 and W_2 :

$$W_0(\theta) = \frac{12\beta\lambda^3}{(1 + 12\lambda^2)\chi(k_i^N) + 12\alpha\lambda^4}, \tag{27}$$

$$W_1(\theta) = \cosh(\eta_i^N\theta) \cos(\zeta_i^N\theta), \tag{28}$$

$$W_2(\theta) = \sinh(\eta_i^N\theta) \sin(\zeta_i^N\theta), \tag{29}$$

where η_i^N, ζ_i^N are obtained from the material constants and satisfy the characteristic equations, namely

$$\eta_i^N = \frac{\sqrt{\sqrt{1 + 12\lambda^2 + \frac{12\alpha\lambda^4}{\chi(k_i^N)}} - 1}}{\sqrt{2}}, \tag{30}$$

$$\zeta_i^N = \frac{\sqrt{\sqrt{1 + 12\lambda^2 + \frac{12\alpha\lambda^4}{\chi(k_i^N)}} + 1}}{\sqrt{2}}. \tag{31}$$

Thus we denote the solution on $[-T/2, T/2]$ as w_T , where the dependence in T is contained in the coefficients A_1, A_2 as follows. Let

$$w_T(\theta) = W_0 + A_1(T)W_1(\theta) + A_2(T)W_2(\theta). \tag{32}$$

A computed example of the solution is plotted in Fig. 2. Nonetheless, the constants A_1, A_2 are obtained from the boundary conditions:

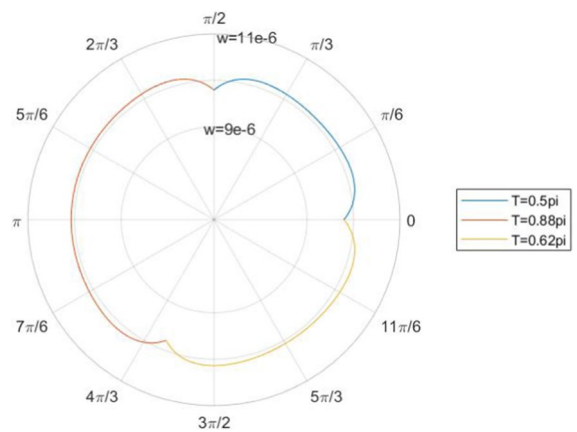


Fig. 2 The displacement fields on a ring with cracks at $0, \pi/2, 1.08\pi$ computed according to (24), (25) and (26). The center angles for each piece are displayed in the legend. Parameters $\alpha = 1e^{-8}, \lambda = 10, \chi(i, N) = 1, \beta = 1e^{-6}$. At cracks the displacement field is discontinuous, hence the regularity of w is not C^0

$$W_0 + A_1(W_1(T/2) + W_{1,\theta\theta}(T/2)) + A_2(W_2(T/2) + W_{2,\theta\theta}(T/2)) = 0, \tag{33}$$

$$A_1(W_{1,\theta}(T/2) + W_{1,\theta\theta\theta}(T/2)) + A_2(W_{2,\theta}(T/2) + W_{2,\theta\theta\theta}(T/2)) = 0, \tag{34}$$

and we easily see that A_1, A_2 are proportional to W_0 hence β .

Recall now the expression of the bulk energy Ψ in (17). At the stage with N cracks, let Ψ_i^{N, T_i} denote the bulk energy associated with the fragment with central angle T_i starting at θ_i^N :

$$\Psi_i^{N, T_i} = \int_{-T_i/2}^{T_i/2} \left\{ 6\alpha\lambda^4 w_T^2 - 12\beta\lambda^3 w_T + \chi(k_i^N) \left(6\lambda^2 w_T^2 + \frac{1}{2}(w_T + w_{T,\theta\theta})^2 \right) \right\} d\theta. \tag{35}$$

And for $N = 0, \Psi_0^{0, 2\pi}$ is given by taking $T = \pi$ and substituting the particular (constant) solution (27), i.e. $w_T = W_0$ into (35).

Now substitute (32) and the values of the constants A_1 and A_2 into (35) to obtain

$$\Psi_i^{N, T_i} = a(T_i, k_i^N)\beta^2, \tag{36}$$

where the function $a(., k_i^N)$ depends (in background) exclusively on the length of the unbroken piece and the evolution that produced the given piece, at fixed material parameters. In this way the bulk energy of the ring with N segments, denoted to Ψ^N , reads

$$\Psi^N = \sum_{i=1}^N \Psi_i^{N, T_i} = \beta^2 \sum_{i=1}^N a(T_i, k_i^N). \tag{37}$$

Note that the bulk energy is quadratic in β and $a(T_i, k_i^N)$ is constant between cracking events for all segments. Let $\mathcal{T}^N := \{\theta_{i+1}^N - \theta_i^N\}$ with $\theta_i^N \in \Gamma^N$ and $\theta_{i+1}^N \in \Gamma^N \cup \{2\pi\}$. Our findings so far are summarized in the following lemma:

Lemma 2 *At a given number of cracks N and pressure β , the value of the energy functional depends on the position of the cracks (or lengths of the unbroken pieces) and the evolution that produced the given arrangement in the following fashion:*

$$\mathcal{E}^N = \beta^2 \sum_{i=1}^N a(T_i, k_i^N) + 12N\gamma\lambda = \beta^2 a^N + 12N\gamma\lambda. \tag{38}$$

Here a^N can be computed recursively.

$$\begin{aligned} a^0 &= \frac{\Psi_0^{0, 2\pi}}{\beta^2}, \\ a^1 &= \frac{\Psi_1^{1, 2\pi}}{\beta^2}, \\ a^{N+1} - a^N &= \min_{T \in \mathcal{T}^N, 0 < x < 1} a(Tx, k_i^{N+1}) \\ &\quad + a(T(1-x), k_i^{N+1}) - a(T, k_i^N). \end{aligned} \tag{39}$$

Notice that (38) gives a geometric interpretation to the problem. The energy landscape consists of parabolas whose shape is controlled by the parameter a^N depending exclusively on the geometry and the preceding evolution. The *cracking pressures*, at which a cracking event occurs, are the intersection points of these parabolas.

Lemma 3 *(Possibility of a new crack) If we have followed a quasi-static evolution till the point when there are N cracks, and β is such that*

$$a^N - a^{N+1} = \frac{12\lambda\gamma}{\beta^2}, \tag{40}$$

then a new crack appears.

Proof Let us now consider a cracked set of N cracks Γ_N . We look for a new crack position x satisfying (39). Due to the quasi-static setting, at the cracking value β at which the $N + 1$ -th crack instantaneously opens, we have $\mathcal{E}^N = \mathcal{E}^{N+1}$. Using expression (39) for the coefficients a^N, a^{N+1} defining the energy and the fact that only the last crack position differs due to the irreversibility, plus recalling the translation-invariance gets us to the desired result. \square

Equation (40) lies at the very heart of the cracking process: there cannot be an additional crack as long as the change in the bulk energy associated with every test-crack position is not at least the cracking energy. On the other hand as soon as this condition is satisfied, a new crack opens and we switch from the parabola equation \mathcal{E}^N to the parabola \mathcal{E}^{N+1} . Note that the left-hand side contains on its own all the influence of the geometry and on the p on the possibility to open a new crack, whereas the right-hand side should be understood as some kind of bound that becomes easier to overcome as the pressure β increases.

Note that Eq. (40) might have no solutions if (a^N) is a nondecreasing sequence. We pursue these considerations further in Sect. 3.4.

3.3 Cracking on a single fragment

In this subsection we look into the properties of one unbroken fragment. In particular, we show how to choose the new crack position according to an energy minimality criterion. We show that there exist a critical length above which two possible cracking points coexist, and they merge into one as the length of the unbroken piece shrinks to zero.

Take a cracked set $\Gamma_N = \{\theta_i^N\}_{i=1}^N$. The problem to solve to find a new cracking position is given by (39), and we see that this comes to comparing the results of N instances of the same minimization problem. Namely we investigate the minimization of the following *add-crack energy function*:

$$f_i^N(T, x) = a(T(1-x), k_{i+1}^{N+1}) + a(Tx, k_{i+1}^{N+1}), \tag{41}$$

where $x \in]0, 1[$ represents the relative position on the fragment of length T at which we expect a new crack

to occur. The solution of the minimization for the whole ring (39) will then follow easily by comparing the minimizing values on the set of N unbroken fragments.

Lemma 4 (Critical points of the add-crack energy function) Possible cracking positions for the unbroken piece $[-T/2, T/2]$ with relaxation function value $\chi(k_i^N)$ are to look for among those x such that either

$$w_{T(1-x)}\left(\frac{T(1-x)}{2}\right) - w_{Tx}\left(\frac{Tx}{2}\right) = 0, \tag{42}$$

or

$$w_{T(1-x)}\left(\frac{T(1-x)}{2}\right) + w_{Tx}\left(\frac{Tx}{2}\right) - \frac{2\beta\lambda}{\alpha\lambda^2 + \chi(k_i^N)} = 0. \tag{43}$$

Proof Let us search for critical points. In a first step we find an expression for the derivative of $a(T, k_i^N)$ with respect to T . Recall the expression of $a(T, k_i^N)$ given in Eqs. (35) and (36). An affine variable change allows to write $a(T, k_i^N)$ as an integral expression of the following form:

$$a(T, k_i^N) = T \int_{-1/2}^{1/2} 6\alpha\lambda^4 w_T(\varphi T)^2 - 12\beta\lambda^3 w_T(\varphi T) + \Phi_i^N(w, w_{\theta\theta})(T, \varphi T) d\varphi. \tag{44}$$

We can differentiate this expression with respect to T and rearrange to obtain the following:

$$\begin{aligned} \frac{\partial a(T, k_i^N)}{\partial T} &= \frac{a(T, k_i^N)}{T} \\ &+ \int_{-1/2}^{1/2} w_{T,T}(\varphi T) \left(\frac{\partial \Phi_i^N}{\partial w}(w_T, w_{T,\theta\theta})(\varphi T) \right. \\ &+ 12\alpha\lambda^4 w_T(\varphi T) - 12\beta\lambda^3 \Big) \\ &+ w_{T,\theta\theta T}(\varphi T) \frac{\partial \Phi_i^N}{\partial w_{\theta\theta}}(w_T, w_{T,\theta\theta})(\varphi T) d\varphi + \end{aligned} \tag{45}$$

$$\begin{aligned} \frac{1}{T} \int_{-1/2}^{1/2} \varphi \frac{d}{d\varphi} (6\alpha\lambda^4 w_T^2(\varphi T) - 12\beta\lambda^3 w_T(\varphi T) \\ + \Phi_i^N(w_T, w_{T,\theta\theta})(\varphi T)) d\varphi. \end{aligned} \tag{46}$$

After two integrations by part the first integral (45) is just the integral of (24) and some terms that vanish from the boundary conditions (25), (26). Another integration by part in (46) and using the boundary conditions again considerably simplifies the result namely

$$\begin{aligned} \frac{\partial a(T, k_i^N)}{\partial T} &= 6\alpha\lambda^4 w_T\left(\frac{T}{2}\right)^2 \\ &- 12\beta\lambda^3 w_T\left(\frac{T}{2}\right) + 12\alpha\lambda^4 w_T\left(\frac{T}{2}\right). \end{aligned} \tag{47}$$

The second step is to differentiate f_i^N . Recalling its expression (41), differentiating with respect to x , substituting (47), taking into account the boundary condition (25) and factorizing yields the claim of the lemma. \square

Now that we have a characterization of the critical points, let us look at what happens in practice when the unbroken segment of angular length T is to undergo fracture. We start by looking at the possible cracking points by investigating the criticality conditions. We first show a useful property of the solution that makes Lemma 4 more exploitable.

Lemma 5 (Solution values at endpoints) The solution of the problem (24) on $[-T/2, T/2]$ with boundary conditions (25), (26) and relaxation function value $\chi(k_i^N)$ has the following value at $\pm T/2$:

$$w_T(T/2) = K_i^N \frac{\zeta_i^N \sin(\zeta_i^N T) + \eta_i^N \sinh(\eta_i^N T)}{\eta_i^N \sin(\zeta_i^N T) + \zeta_i^N \sinh(\eta_i^N T)}, \tag{48}$$

where

$$\begin{aligned} K_i^N &= \sqrt{\frac{12\beta^2\lambda^4}{(\chi(k_i^N) + \alpha\lambda^2)(12\alpha\lambda^4 + (1 + 12\lambda^2)\chi(k_i^N))}}. \end{aligned} \tag{49}$$

Proof Recall equations (33), (34). Solving for A_1 and A_2 is straightforward. Plugging the result into (32), substituting (27), (28) and (29) and making good use of circular and hyperbolic trigonometry formulas yields the result. \square

With the previous lemma in hand we can get a great deal of information about the behavior of the

system. In particular, we see that the second criticality condition (43) is never fulfilled: (42) gives all the critical points. The condition (42) is easily seen to be equivalent to finding the roots of the following *criticality function*

$$c_i^N(T, x) = \sin(\zeta_i^N Tx) \sinh(\eta_i^N T(1 - x)) - \sin(\zeta_i^N T(1 - x)) \sinh(\eta_i^N Tx). \tag{50}$$

It is sufficient to investigate $x \in]0, 1[$. We consider T as a parameter for the time being.

Theorem 1 (*Small fragments: the halving rule*) *There exists an angle value T_c such that, if every consecutive crack positions $\theta_i^N, \theta_{i+1}^N$ in the cracked set Γ^N satisfy $\theta_{i+1}^N - \theta_i^N \leq T_c$, then cracking occurs at the middle of one of the current unbroken pieces.*

Proof We are looking at solutions x of (42). We study rather the roots of the criticality function (50). That is we look for solutions x of:

$$\sin(\zeta_i^N Tx) \sinh(\eta_i^N T(1 - x)) - \sin(\zeta_i^N T(1 - x)) \sinh(\eta_i^N Tx) = 0, \tag{51}$$

where we see T as a parameter. Consider now small lengths T . The left hand side can be expanded at 4th order in T to obtain

$$\begin{aligned} & \sin(\zeta_i^N Tx) \sinh(\eta_i^N T(1 - x)) - \sin(\zeta_i^N T(1 - x)) \sinh(\eta_i^N Tx) \\ &= \frac{(\zeta_i^N)^4 - (\eta_i^N)^4}{3!} T^4 \zeta_i^N \eta_i^N x(1 - x)((1 - x)^2 - x^2) + o(T^4). \end{aligned} \tag{52}$$

And this expression cannot be zero except for $x = 1/2$, as the values $x = 0$ or $x = 1$ are prohibited. \square

This means that as soon as the ring is composed of uniformly small fragments, every further crack will appear at the middle of one of the existing fragments. From that point we know exactly how the cracking pattern will evolve: every piece will follow a halving rule. We complete it with the behavior of the system when there exist longer fragments.

Theorem 2 (*Pattern bifurcation*) *Consider the problem of finding the new cracking position for an*

unbroken piece $[0, L]$. The add-crack energy function minimum undergoes a supercritical pitchfork bifurcation at T^ .*

1. If $T < T^*$, the midpoint of the unbroken piece is the only global minimum.
2. If $T > T^*$, there are two global minima, their position is symmetrical w.r.t the midpoint of the fragment.

Proof Recall that for a given piece defined by an angle T , the midpoint $x = 1/2$ is a critical point of the add-crack energy function. Searching for more possible critical points, we look at the behavior of c_i^N in the vicinity of the midpoint, so we let $x = 1/2 \pm \delta x$ in (42) and expand at third order in δx around $T/2$. After using the criticality of $x = 1/2$ for c_i^N we have two equations.

$$c_i^N(T, \frac{1}{2} + \delta x) = \delta x c_{i,x}^N(T, 1/2) + \frac{\delta x^2}{2} c_{i,xx}^N(T, 1/2) + \frac{\delta x^3}{3!} c_{i,xxx}^N(T, 1/2) + o(\delta x^3), \tag{53}$$

$$c_i^N(T, \frac{1}{2} - \delta x) = -\delta x c_{i,x}^N(T, 1/2) + \frac{\delta x^2}{2} c_{i,xx}^N(T, 1/2) - \frac{\delta x^3}{3!} c_{i,xxx}^N(T, 1/2) + o(\delta x^3). \tag{54}$$

From the symmetry of the system these two should be equal so their difference is zero. After ruling out $\delta x = 0$ we ask if there are solutions to the following:

$$\frac{\delta x^2}{3!} c_{i,xxx}^N(T, 1/2) = c_{i,x}^N(T, 1/2). \tag{55}$$

The possibility for nontrivial solutions is given by the sign of the ratio $c_{i,x}^N(T, 1/2)/c_{i,xxx}^N(T, 1/2)$: two additional solutions if it is positive and none if it is negative. A plot here way more insightful than a long calculation. According to Figs. 3 and 4, we get that there is a sign change at some critical angle T^* . So there is more than one candidates for cracking positions as long as the unbroken piece is long enough.

Looking at the minimality, we realize that for small unbroken fragments $T < T^*$, only the midpoint is a global minimizing position. On the other hand for long fragments, there are two global minima, symmetrical with respect to the midpoint. \square

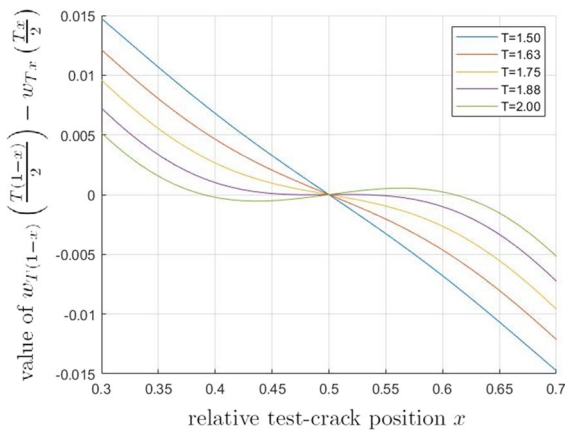


Fig. 3 Value of the critical condition (42) against relative position on the unbroken piece for the set of parameters $\lambda = 10, \alpha = 1e^{-8}, \chi(i, N) = 0.992$ and different lengths. Note the bifurcation between $T = 1.5$ and $T = 2$: as L increases the number of roots increases from 1 to 3. The second order minimality condition can be seen from the sign of the derivative at the roots. As the bifurcation occurs, the slope at the position $x = 1/2$ switches from negative for lengths $T \leq 1.88$ to positive for lengths $T \geq 1.88$, making the middle point from a minimum a maximum

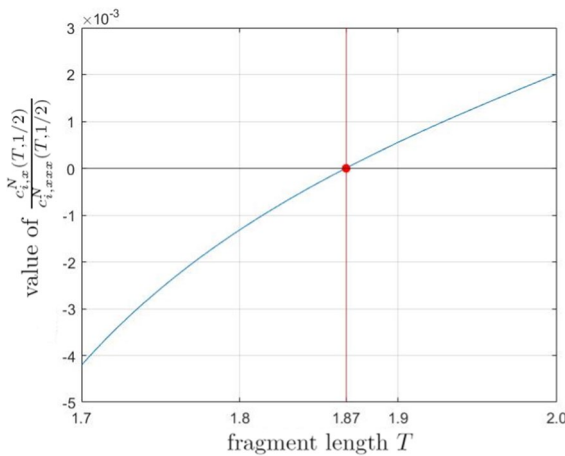


Fig. 4 The value of the ratio of the first to third derivatives of c_1 for $1.5 \leq T \leq 2$ for the set of parameters $\lambda = 10, \alpha = 1e^{-8}, \chi(i, N) = 0.992$. Observe the expected change of sign in the first to third derivative ratio as given in (55) and seen in Fig. 3. We get a value for the bifurcation at $T^* \approx 1.87$

Finally we give some bounds on the length of the fragment T^* where the system undergoes bifurcation.

Theorem 3 (Bifurcation position) *We have the following bounds for T^* :*

$$\frac{5\pi}{2\zeta_i^N} < T^* < \frac{5\pi}{2\eta_i^N}. \tag{56}$$

With ζ_i^N, η_i^N given (31), (30) and depending on the slenderness λ , the spring rigidity α and the value of the relaxation $\chi(k_i^N)$.

Proof Recall the definition of the criticality function c_i^N from (50).

$$c_i^N(T, x) = \sin(\zeta_i^N Tx) \sinh(\eta_i^N T(1-x)) - \sin(\zeta_i^N T(1-x)) \sinh(\eta_i^N Tx).$$

From the symmetry we can restrict ourselves to $x \in]0, 1/2[$.

The upper bound is proved by setting $T = 5\pi/(2\eta_i^N)$ and showing that there exist roots of c_i^N in $]0, 1/2[$. We may equivalently factor an hyperbolic sine out and show that there exist roots of

$$\tilde{c}_i^N = \sin(\zeta_i^N Tx) - \sin(\zeta_i^N T(1-x)) \frac{\sinh(\eta_i^N Tx)}{\sinh(\eta_i^N T(1-x))}. \tag{57}$$

It is straightforward that

$$\lim_{x \rightarrow 0} \tilde{c}_i^N(T, x) = \lim_{x \rightarrow 1/2} \tilde{c}_i^N(T, x) = 0. \tag{58}$$

Differentiating \tilde{c}_i^N yields:

$$\begin{aligned} \tilde{c}_{i,x}^N(T, x) &= \zeta_i^N T \cos(\zeta_i^N Tx) \zeta_i^N T \\ &\quad + \cos(\zeta_i^N T(1-x)) \frac{\sinh(\eta_i^N Nx)}{\sinh(\eta_i^N T(1-x))} \\ &\quad - \eta_i^N T \sin(\zeta_i^N T(1-x)) \frac{\sinh(\eta_i^N T)}{\sinh(\eta_i^N T(1-x))^2}. \end{aligned} \tag{59}$$

Let us examine the limits of the derivatives on the boundaries of the interval. We have easily the sign around zero:

$$\lim_{x \rightarrow 0} \tilde{c}_{i,x}^N(x) = \zeta_i^N T \left(1 - \frac{\eta_i^N \sin(\zeta_i^N T)}{\zeta_i^N \sinh(\eta_i^N T)} \right) > 0. \tag{60}$$

After taking a series expansion and factorizing around $x = 1/2$ we find

$$\begin{aligned} &\lim_{x \rightarrow 1/2} \tilde{c}_{i,x}^N(x) \\ &= \sum_{k \geq 0} \frac{(-1)^k}{(2k)!} \left(\frac{\pi \zeta_i^N}{4 \eta_i^N} \right)^{2k} \left(2 - \frac{5\pi}{4(2k+1) \sinh(5\pi/4)} \right), \end{aligned} \tag{61}$$

which is easily verified to be an alternating series, hence positive like its first term. Now we see that $\tilde{c}_{i,x}^N$ is positive close to $x = 0$ and $x = 1/2$. This means \tilde{c}_i^N is positive next to $x = 0$ and negative next to $x = 1/2$. The intermediate values theorem allows to conclude the existence of a root for \tilde{c}_i^N , thus for c_i^N .

For the lower bound, we have to prove that for all $0 < T < \frac{5\pi}{2\zeta_i^N}$, the criticality function has no zero in $]0, 1/2[$.

First we show the bound for $0 < T \leq \frac{2\pi}{\zeta_i^N}$. We will use the product expansions of sinh and sin

$$\sinh(\eta_i^N Tx) = x \prod_{n \geq 1} \left(1 + \frac{(\eta_i^N Tx)^2}{\pi^2 n^2} \right), \tag{62}$$

$$\sin(\zeta_i^N Tx) = x \prod_{n \geq 1} \left(1 - \frac{(\zeta_i^N Tx)^2}{\pi^2 n^2} \right). \tag{63}$$

Substituting in (50) and factoring yields the following expression for c_i^N :

$$\begin{aligned} c_i^N(x) &= (x(1-x)\zeta_i^N \eta_i^N T^2)^2 \\ &\times \left(\prod_{n \geq 1} \left(1 - \frac{(\zeta_i^N Tx)^2}{(\pi n)^2} \right) \left(1 + \frac{(\eta_i^N T(1-x))^2}{(\pi n)^2} \right) \right. \\ &\left. - \prod_{n \geq 1} \left(1 - \frac{(\zeta_i^N T(1-x))^2}{(\pi n)^2} \right) \left(1 + \frac{(\eta_i^N Tx)^2}{(\pi n)^2} \right) \right). \end{aligned} \tag{64}$$

The first sum is strictly positive from the hypothesis on T . Factoring reduces the study of the sign of c_i^N to that of

$$1 - \prod_{n \geq 1} \frac{\left(1 - \frac{(\zeta_i^N T(1-x))^2}{(\pi n)^2} \right) \left(1 + \frac{(\eta_i^N \pi x)^2}{(\pi n)^2} \right)}{\left(1 - \frac{(\zeta_i^N Tx)^2}{(\pi n)^2} \right) \left(1 + \frac{(\eta_i^N \pi(1-x))^2}{(\pi n)^2} \right)}. \tag{65}$$

It is easy to see that for $0 < T < \frac{2\pi}{\zeta_i^N}$, for all $0 < x < 1/2$, each term in the product on the right is strictly smaller than 1 and positive but two. That is however not a problem because these two terms belong to the same product, and we conclude that $c_i^N > 0$ on $]0, 1/2[$.

Now for $\frac{2\pi}{\zeta_i^N} < T < \frac{5\pi}{2\zeta_i^N}$, the previous method applies to $0 < x < \frac{\pi}{\zeta_i^N T}$. However, it fails for other x because there are two negative terms not in the same product. So let $\frac{\pi}{\zeta_i^N T} < x < \frac{1}{2}$. The fact that there is no zero for x on this interval reduces to showing that for all x

$$\frac{\sin(\zeta_i^N T(1-x))}{\sin(\zeta_i^N Tx)} < \frac{\sinh(\eta_i^N T(1-x))}{\sinh(\eta_i^N Tx)}. \tag{66}$$

The derivative on the left hand side is easily seen to be $-\frac{\zeta_i^N T}{\sin(\zeta_i^N Tx)} > 0$, whereas that of the right hand side is $-\frac{\eta_i^N T}{\sinh(\eta_i^N Tx)} < 0$. Further, these two terms both have limit 1 when $x \rightarrow \frac{1}{2}$. The inequality is true in the range considered, and we have the bound announced. \square

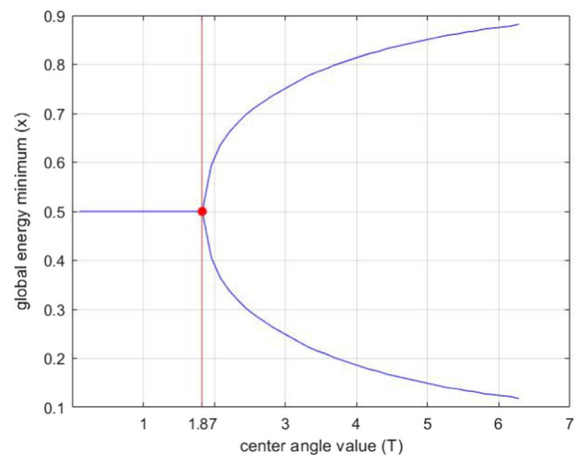


Fig. 5 The plot of a bifurcation diagram with the parameters $\lambda = 10, \alpha = 1e^{-8}, \chi = 0.992$. In blue, the crack position minimizing the energy as a function of the length of the piece. Observe the bifurcation at $T \approx 1.87$ as expected from Fig. 4

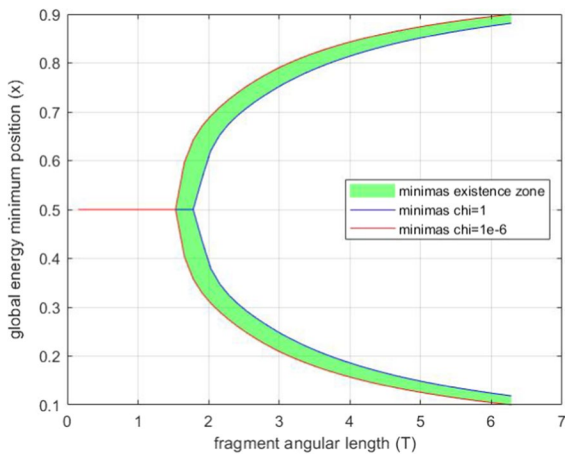


Fig. 6 The minimas existence zone for $\lambda = 10$, $\alpha = 1e^{-8}$. As the evolution goes on for the whole ring, relaxation takes place over the different fragments and the relative cracking position will remain in the green zone for all fragments where $1e - 6 < \chi < 1$. The influence of the relaxation becomes noticeable only when $1 + 12\lambda^2$ is of the same order of magnitude as $12\lambda^4/\chi$

With this in hand we know exactly where a crack will open on one fragment. For long fragments, cracking occurs next to the edge till the fragment reaches the critical length T^* , after what cracking occurs according to the halving rule. The bifurcation occurring at T^* is depicted in Fig. 5. The variation of the bifurcation diagram as the relaxation takes place is shown on Fig. 6. Examples of the full evolution are given in Sect. 4.

3.4 Cracking pressure, homogeneity

In this subsection we examine the problem (38), (39) for the cracking of the whole ring. In particular we show that cracking occurs always on the longest fragment and derive the expression for $\beta_{N,N+1}$ at which the $N + 1$ th crack opens. Finally, we discuss the requirements a^N should satisfy to ensure a "well-behaved" evolution.

Recall Eq. (38) and that a^N are defined recursively from the add-crack energy function $f_i^N(L, x)$ (41) and the size of the ring fragments $T_N = \{\theta_{i+1} - \theta_i, \theta_i, \theta_{i+1} \in \Gamma_N \cup \{2\pi\}\}$. Under the form (38), the energy minimization is exactly a segmentation problem, and we refer for instance to [23] for an introduction to the subject.

The energy \mathcal{E}^N against β curves are parabolas whose shape is given by the value of the coefficient a^N , as a byproduct of the minimization of the energy w.r.t. the crack positions. As β increases and we follow a quasi-static evolution path, the number of cracks gradually increases and the energy minimization follows a path given by sections of the parabolas $\mathcal{E}^0, \dots, \mathcal{E}^N$. For a new crack to occur we have to be at the intersection point of curves \mathcal{E}^N and \mathcal{E}^{N+1} , thus the pressure at which the $(N + 1)$ th crack occurs satisfies

$$(a^N - a^{N+1})\beta_{N,N+1}^2 = 12\lambda\gamma. \tag{67}$$

Equation (67) defines $\beta_{N,N+1}$ uniquely on $\mathbb{R}^+ \cup \infty$ as long as there is a solution. For a solution to exist it is sufficient to verify that (a^N) is a decreasing sequence.

Lemma 6 (Existence of the cracking pressure) *The sequence (a^N) is decreasing. That is to say for all N , there is a value $\beta_{N,N+1} \in \mathbb{R}^+$ such that $\mathcal{E}^N(\beta_{N,N+1}) = \mathcal{E}^{N+1}(\beta_{N,N+1})$.*

Proof Two linear changes of variables $\theta = \varphi/x$, $\theta = \varphi/(1 - x)$ allow to write the quantity to be minimized (39) as

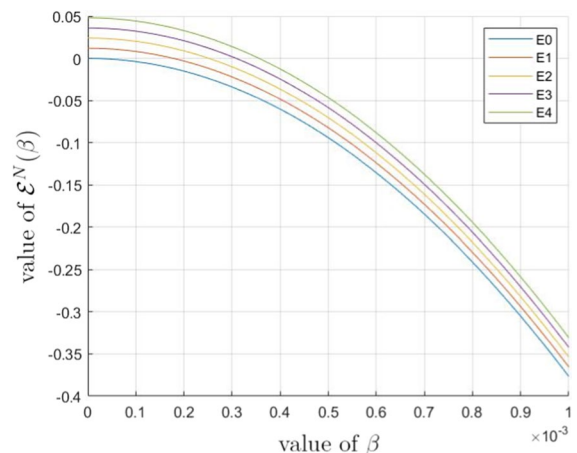


Fig. 7 Plot of the energy trajectories $\mathcal{E}^N(\beta)$, $0 \leq N \leq 4$ for the parameter set $\lambda = 10$, $\alpha = 1e^{-8}$, $\gamma = 1e^{-4}$, $\delta\chi = 1e^{-3}$ on the range $\beta \in [0, 1e^{-3}]$. Notice the evolution according to Lemma 6. On the range of β considered here, the uncracked solution is the global minimizer. The parabolas intersect at a slightly higher pressure, leading to the cracked solutions being energetically more favorable, see Fig. 8

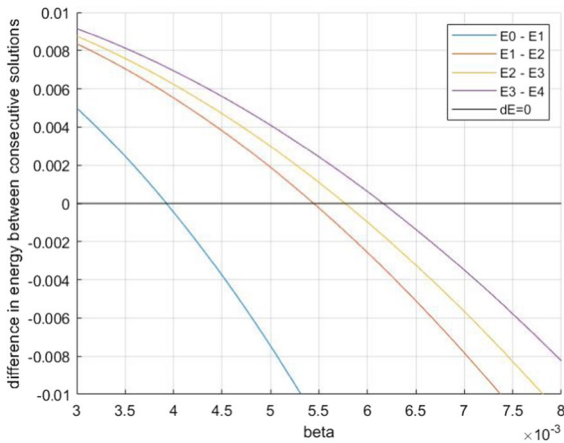


Fig. 8 Plot of the difference of the energies $\mathcal{E}^{N+1} - \mathcal{E}^N$, $0 \leq N \leq 4$ for the parameter set $\lambda = 10, \alpha = 1e^{-8}, \gamma = 1e^{-4}, \delta\chi = 1e^{-3}$ on the range $\beta \in [0, 8e^{-3}]$. The cracking pressures can be seen from the intersections of the plotted curves with the abscissas (black curve). The numerical result in accordance with Lemma 8: the sequence of the cracking pressures increases

$$\min_{0 < x < 1} a(T, k_{i+1}^{N+1}) - a(T, k_i^N). \tag{68}$$

The result follows from $\chi(k_i^N)$ decreasing with N . □

An example can be seen in Figs. 7 and 8. Now we show that up to a correct choice of the relaxation parameter, it is always the longest piece that cracks. This has a very simple meaning. If cracking dissipate most of the strain energy in one piece, then this piece will no longer be a good candidate for cracking, hence favoring less relaxed fragments. The relaxation has to be chosen with care.

Lemma 7 *Provided $\delta\chi$ is small enough, cracking always occur on the longest piece, at least till rank N_0 .*

Proof Lets us consider two angles $T_1 > T_2$ defining two ring fragments with respective relaxation values $\chi(k_i^N), \chi(k_j^N)$. A linear change of variables allows to bring the integrals defining the coefficients on the same interval:

$$\begin{aligned} & a(T_1x, k_{i+1}^{N+1}) + a(T_1(1-x), k_{i+1}^{N+1}) - a(T_1, k_i^N) \\ &= \frac{T_1}{T_2} \left(a(T_2x, k_{j+1}^{N+1}) + a(T_2(1-x), k_{j+1}^{N+1}) - a(T_2, k_j^N) \right) \\ &+ \frac{(j-i)\delta\chi T_1}{T_2} \left(\int_{-T_2x/2}^{T_2x/2} \Phi_{j-i}^N(w_{T_2x}, w_{T_2x,\theta\theta}) d\varphi \right. \\ &+ \int_{-T_2(1-x)/2}^{T_2(1-x)/2} \Phi_{j-i}^N(w_{T_2(1-x)}, w_{T_2(1-x),\theta\theta}) d\varphi \\ &\left. - \int_{-T_2/2}^{T_2/2} \phi_{j-i}^N(w_{T_2}, w_{T_2,\theta\theta}) d\varphi \right). \end{aligned} \tag{69}$$

Now $T_1 > T_2$ and the terms on the first four lines are negative after minimizing. Pick $\delta\chi$ small enough according to (69) to set N_0 . □

Finally, we ensure that the cracking is progressive. The relaxation induces energy dissipation, and we want to avoid the undesirable behavior where the relaxation dissipate so much energy that the system becomes unstable and cracks forever. We show that if the relaxation parameter is small enough, then this behavior can be prohibited.

Lemma 8 *(Monotonicity of the cracking pressure) If $\delta\chi$ is small enough, then the sequence $(a^N - a^{N+1})$ is decreasing at least till some rank N_0 i.e. the sequence of the cracking pressures $\beta_{N,N+1}$ is increasing till rank N_0 .*

Proof Denote by T_N, x_N the length and relative positions that define $a^N - a^{N+1}$ as in the proof of Lemma 6. From our definition of the cracked set, $T_{N+1} < T_N$, as the cracking reduces the size of the longest fragment, and the cracking takes place on this longest fragment. Now we use the fact that $a^N - a^{N+1}$ and $a^{N+1} - a^{N+2}$ solve the same variational problem. From the definition of the coefficients (39) and an affine variable change $\varphi = \frac{T}{T_N}\theta$ in the definition of the coefficients we see

$$\begin{aligned}
 & (a^{N+1} - a^{N+2}) - (a^N - a^{N+1}) \\
 &= -\frac{\delta\chi T_{N+1}}{T_N} \left(\int_{-T_N x/2}^{T_N x/2} \Phi_i^N(w_{T_N x}, w_{T_N x, \theta\theta}) \left(\frac{T_N \varphi}{T_{N+1}}\right) d\varphi \right. \\
 & \quad + \int_{-T_N(1-x)/2}^{T_N(1-x)/2} \Phi_i^N(w_{T_N(1-x)}, w_{T_N(1-x), \theta\theta}) \left(\frac{T_N \varphi}{T_{N+1}}\right) d\varphi \\
 & \quad \left. - \int_{-T_N/2}^{T_N/2} \Phi_i^N(w_{T_N}, w_{T_N, \theta\theta}) \left(\frac{T_N \varphi}{T_{N+1}}\right) d\varphi \right) \\
 & \quad - \frac{T_N - T_{N+1}}{T_N} (a^N - a^{N+1}).
 \end{aligned} \tag{70}$$

From Lemma 6, (a^N) is decreasing so by picking $\delta\chi$ small enough according to (70), we can ensure that the right hand side is negative. \square

Summing up everything about the evolution of the system in the $\beta - \mathcal{E}$ space is straightforward using lemmas 6, 7, 8.

Theorem 4 (System evolution) Consider the problem of cracking of the brittle ring in the quasistatic framework, with energy functional given (16). A $(N + 1)^{\text{th}}$ crack occurs every time the parameter β reaches the value $\beta_{N,N+1}$ given (67).

The evolution of the energy on the range $]\beta_{N-1,N}, \beta_{N,N+1}[$ is given by following the curve \mathcal{E}^N .

4 Numerical simulations

We now turn to numerical implementations of the model and compute the cracking pattern of the brittle ring through the minimization. In order to verify our theoretical results, we perform the calculations as follows. We start with a ring with a single crack at 0 and specify the number of cracks we would like to see at the end of the calculation. From then on, we compute the *add-crack energy function* given (41) for each piece, compute its minimum for each piece, and open the crack according to the global minimization on all the fragments. We verify that the cracking occurs on the longest piece and undergoes bifurcation.

With our range of parameters $\lambda \in \{5, 10, 20\}, \alpha = 1e^{-8}, \delta\chi = 1e - 3$ and the

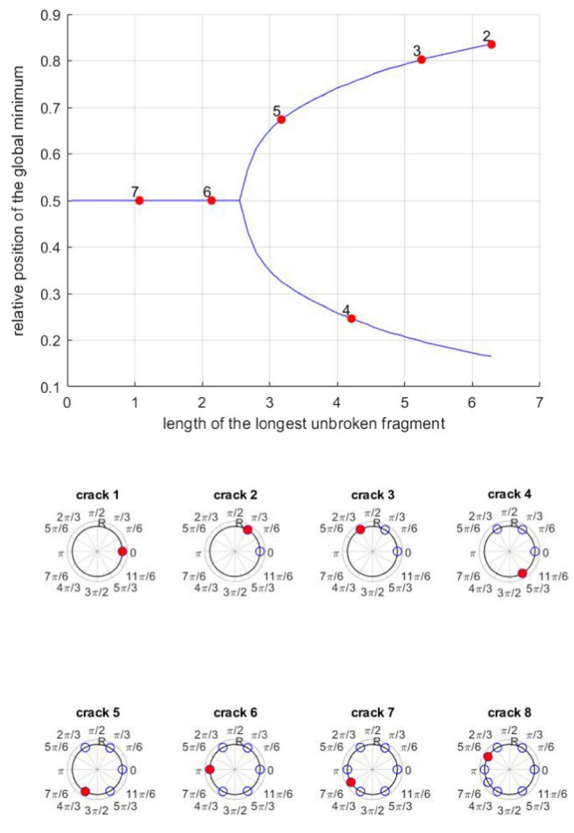


Fig. 9 Bifurcation diagram and first 8 cracks appearing on a brittle ring with parameter $\lambda = 5, \alpha = 1e^{-8}, \delta\chi = 1e^{-3}$. On the crack map, the crack that opens is in red, and its label matches that seen on the bifurcation diagram. Notice the bifurcation and the beginning of the evolution according to the halving rule starting from the 6th crack

number of cracks considered $N < 10$, we have $(1 + 12\lambda^2) \gg (12\lambda^4 / \chi)$, hence existence zone of the minima in green in Fig. 6 is practically reduced to a line.

We plot the computed cracking positions on one bifurcation diagram to verify that they agree. Finally, we plot the cracking pattern as it sequentially appears on the ring.

4.1 Some patterns with the relaxed brittle model, constant spring rigidity

From all the previous results we can readily compute the cracking patterns and verify that they match our expectations.

As expected from Theorem 3, the bifurcation point is displaced to the left when λ increases.

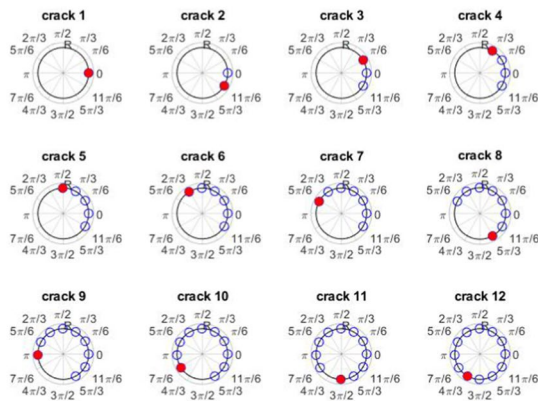
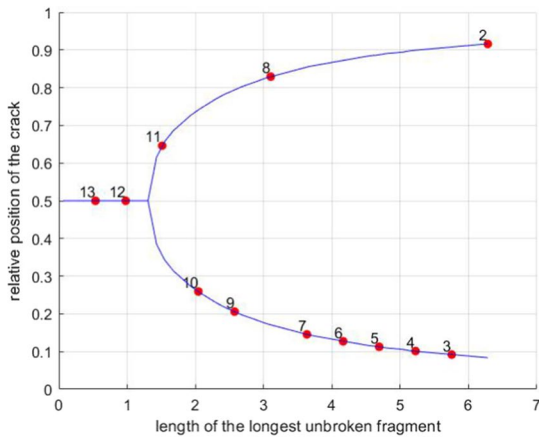


Fig. 10 Bifurcation diagram and first 8 cracks appearing on a brittle ring with parameter $\lambda = 20$, $\alpha = 1e^{-8}$, $\delta\chi = 1e^{-3}$. On the crack map, the crack that opens is in red, and its label matches that seen on the bifurcation diagram. Notice the bifurcation and the beginning of the evolution according to the halving rule starting from the 12th crack

A remarkable feature is that the cracks seem to be equally spaced on the ring, as showed in Figs. 9 and 10. A thorough investigation however shows that the cracking positions are not equally spaced, but *almost* equally spaced. A plausible culprit is the relaxation, that slightly modifies the position of cracking at every step.

4.2 Some patterns with the relaxed brittle model, varying spring rigidity

In practice, we expect the strength of the support, hence α to vary around the circumference of the ring. Such a variation can be used to model various supports for the ring. A simple model for a rigidity

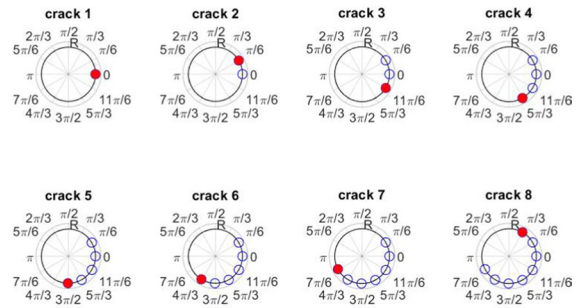


Fig. 11 Plot of the crack map obtained with a rigidity function $\alpha(\theta) = 1e^{-8}(1 + \cos(3\theta))$ and parameters $\lambda = 20, \delta\chi = 1e^{-3}$. Notice that the evolution is similar to that with a constant rigidity: cracks appear regularly spaced

function α can be the sum of a constant and a periodic sine wave function:

$$\alpha(\theta) = \alpha_0 + \alpha_k \sin(k\theta). \tag{71}$$

Our model allows for the computation of the cracking pattern with such an α , but our theoretical results only partially preserved. We show that some of the pattern properties are shared between the models with constant or periodic α . It is however not so easy to describe how the cracks will arrange as a pattern, as the location of the critical points of α essentially influences the emerging pattern. Nonetheless, small variation in α keeps the qualitative picture outlined above, see Fig. 11. A significant perturbation, on the other hand, leads to a more sophisticated evolution (see Fig. 12), as at the maxima of α cracks tend to appear. This numerical example highlights the need

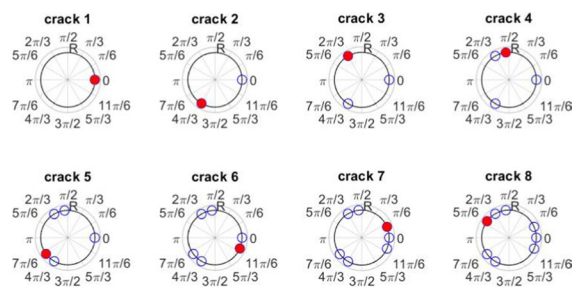


Fig. 12 Plot of the crack map obtained with a rigidity function $\alpha(\theta) = 1e^{-4}(1 + \cos(3\theta))$ and parameters $\lambda = 20, \delta\chi = 1e^{-3}$. Cracks 2 and 3 appear at maxima of the rigidity, then start to appear at regular distances

for extra care, either the crack evolution in an experiment, or an existing monument is analyzed.

5 Conclusion

A simple, quasi-static model to investigate the evolution of the cracking pattern of brittle, pressurized rings constrained by radial elastic springs in the plane is introduced. The elastic energy of the fragments are relaxed upon a cracking event. The minimization of the Griffith energy functional associated with the problem leads to a simultaneous solution of Boundary Value Problems associated with the minimal energy of the unbroken fragments.

The existence of solutions in the framework of Γ -convergence is proved. The problem is then investigated with a constant spring rigidity as a sequence of minimizations leading to a sequential cracking. We find, that the location of the emerging cracks is eminently driven by internal bending, whereas the load level, at which a cracking event occur is due to the dominant tension in the ring. The main finding of the paper is the identification of a codimension-one bifurcation in the location of the cracking positions. In specific, we show that sufficiently short fragments follow a halving rule, whereas for long fragments the model predict cracking in the vicinity of an existing crack. The sizes at which this bifurcation in the behavior of the system occurs is investigated and bounds on the size of the piece at which the bifurcation occurs are given.

Considering an energetic vantage point, the order of the cracking sequence is investigated. The cracking pressure allowing to open a new crack is computed and under mild assumptions on the relaxation parameter, the model is proved to be consistent with the natural expectation that cracking events are driven by an increase in the internal pressure.

Finally, numerical simulations comfort the findings and reveal that the pattern formation consists of two phases, as it is predicted by the bifurcation in the behavior of the system. In a first phase, cracks develop at a regular (but not equal) distance from each other till all the fragments of the ring are uniformly small, after what they follow a halving rule. Additional simulations with periodic spring rigidity show that the behavior in this more general case partially share features of the constant spring

model, although the cracking pattern inherits some properties of the rigidity function.

The presented model can serve as a simple explanation for the crack evolution in vertically loaded, symmetric hemispherical domes, a distinguished problem of structural mechanics. One might argue that, in principle, the dome cracking happens due to the tensile hoop stress apparent at the lower regions of the dome, which can be modeled with the pressurized brittle ring. The predicted crack evolution in our model, namely the tendency of cracks appearing close to each other as long as there are a few of them, and the tendency to follow the halving rule in the presence of more than 5–7 cracks, apart from stochastic noise, is in accordance with experimental data [24]. There, the crack evolution of hemispherical specimens is reported. The applicability and the limitations of the presented model for the study of hemispherical domes hence is a promising topic for future research.

Acknowledgements The research was supported by the NKFIH Grant 134199 and by the TKP2021-BME-NVA-02 program.

Funding Open access funding provided by Budapest University of Technology and Economics.

Declarations

Conflict of interest The authors declare that they have no conflict of interest.

Open Access This article is licensed under a Creative Commons Attribution 4.0 International License, which permits use, sharing, adaptation, distribution and reproduction in any medium or format, as long as you give appropriate credit to the original author(s) and the source, provide a link to the Creative Commons licence, and indicate if changes were made. The images or other third party material in this article are included in the article's Creative Commons licence, unless indicated otherwise in a credit line to the material. If material is not included in the article's Creative Commons licence and your intended use is not permitted by statutory regulation or exceeds the permitted use, you will need to obtain permission directly from the copyright holder. To view a copy of this licence, visit <http://creativecommons.org/licenses/by/4.0/>.

References

1. Angelier J (1984) Tectonic analysis of fault slip data sets. *J Geophys Res* 89:5835–5848

2. Heyman J (1995) *The stone skeleton: structural engineering of masonry architecture*. Cambridge University Press, Cambridge
3. Griffith AA (1921) VI. The phenomena of rupture and flow in solids. *Philos Trans R Soc Lond Ser A* 221(582–593):163–198
4. Barenblatt GI (1962) The mathematical theory of equilibrium cracks in brittle fracture. *Adv Appl Mech* 7:5–129
5. Gross D, Seelig T (2018) *Fracture mechanics. With an introduction to micromechanics*, 3rd edn. Springer, Berlin
6. Francfort GA, Marigo JJ (1998) Revisiting brittle fracture as an energy minimization problem. *J Mech Phys Solids* 46(8):1319–1342
7. Dal Maso G, Toader R (2002) A model for the quasi-static growth of brittle fractures based on local minimization. *Math Models Methods Appl Sci* 12(12):1773–1799
8. Dal Maso G, Francfort GA, Toader R (2005) Quasistatic crack growth in nonlinear elasticity. *Arch Ration Mech Anal* 176(2):165–225
9. Marigo JJ, Maurini C, Pham K (2016) An overview of the modelling of fracture by gradient damage models. *Meccanica* 51:3107–3128
10. Kawamura H, Hatano T, Kato N, Biswas S, Chakrabarti BK (2012) Statistical physics of fracture, friction, and earthquakes. *Am Phys Soc* 84(2):839–884
11. Domokos G, Jerolmack DJ, Kun F, Török J (2020) Plato's cube and the natural geometry of fragmentation. *Proc Natl Acad Sci* 117(31):18178–18185
12. Masi F, Stefanou I, Vannucci P (2018) On the origin of the cracks in the dome of the Pantheon in Rome. *Eng Fail Anal* 92:587–596
13. Banichuk NV, Barthold FJ, Serra M (2005) Optimization of axisymmetric membrane shells against brittle fracture. *Meccanica* 40:135–145
14. Bourdin B (2007) Numerical implementation of the variational formulation for quasi-static brittle fracture. *Interfaces Free Bound* 9(3):411–430
15. Bourdin B, Francfort GA, Marigo JJ (2008) The variational approach to fracture. *J Elast* 91(1–3):5–148
16. Lai W, Gao J, Li Y, Arroyo A, Shen Y (2020) Phase field modeling of brittle fracture in an Euler–Bernoulli beam accounting for transverse part-through cracks. *Comput Methods Appl Mech Eng* 361:112787
17. Tadjbakhsh I, Odeh F (1967) Equilibrium states of elastic rings. *J Math Anal Appl* 18:59–74
18. Antman SS (2005) *Nonlinear problems in elasticity*, 2nd edn. Springer, New York
19. Mumford D, Shah J (1989) Optimal approximations by piecewise smooth functions and associated variational problems. *Commun Pure Appl Math* 42:577–685
20. Blake A, Zisserman A (1987) *Visual reconstruction*. MIT Press, London
21. Bellettini G, Coscia A (1994) Discrete approximation of a free discontinuity problem. *Numer Funct Anal Optim* 15(3–4):201–224
22. Ambrosio L, Faina L, March R (2001) Variational approximation of a second order free discontinuity problem in computer vision. *SIAM J Math Anal* 32(6):1171–1197
23. Braides A (2002) *Gamma-convergence for beginners*, vol 22. Clarendon Press, Oxford
24. Cao S, Sipos AA (2022) Cracking patterns of brittle hemispherical domes: an experimental study. *Frattura ed Integrità Strutturale* 59:265–310

Publisher's Note Springer Nature remains neutral with regard to jurisdictional claims in published maps and institutional affiliations.